JOURNAL OF AGRICULTURAL AND FOOD CHEMISTRY

ARTICLE

pubs.acs.org/JAFC

Andrographolide Inhibits ICAM-1 Expression and NF-κB Activation in TNF-α-Treated EA.hy926 Cells

Che-Yi Chao,[†,∥] Chong-Kuei Lii,[§,∥] I-Ting Tsai,[§] Chien−Chun Li,[#] Kai-Li Liu,[#] Chia-Wen Tsai,[§] and Haw-Wen Chen*[,§]

[†]Department of Health and Nutritional Biotechnology, Asia University, Taichung, Taiwan

[§]Department of Nutrition, China Medical University, Taichung, Taiwan

[#]Department of Nutrition, Chung Shan Medical University, Taichung, Taiwan

Supporting Information

ABSTRACT: Several lines of evidence indicate that inflammation and endothelial cell dysfunction are important initiating events in atherosclerosis. Tumor necrosis factor-α (TNF-α), a pro-inflammatory cytokine, induces the expression of cell adhesion molecules and results in monocyte adherence and atheromatous plaque formation. Andrographolide (AP) is a major bioactive diterpene lactone in *Andrographis paniculata* that has anti-inflammatory activity. A previous study demonstrated the role of heme oxygenase 1 (HO-1) in the inhibition of TNF-α-induced ICAM-1 expression by AP. The present study investigated the effect of AP on the IKK/NF-κB signaling pathway, which mediates TNF-α-induced ICAM-1 expression in EA.hy926 cells. Similar to the previous study, AP inhibited TNF-α-induced ICAM-1 mRNA and protein levels, its expression on the cell surface, and subsequent adhesion of HL-60 cells to EA.hy926 cells. AP inhibited TNF-α-induced κB inhibitor (IκB) kinase (IKK) and IκBα activation, p65 nuclear translocation, NF-κB and DNA binding activity, and promoter activity of ICAM-1. Although AP increased the intracellular cAMP concentration and induced the phosphorylation of cAMP response element-binding protein (CREB), knocking down CREB protein expression by transfecting the cells with CREB-specific small interfering RNA did not relieve the inhibition of ICAM-1 expression by AP. Taken together, these results suggest that AP down-regulates TNF-α-induced ICAM-1 expression at least in part via attenuation of activation of NF-κB in EA.hy926 cells rather than through activation of CREB. The results suggest that AP may have potential as a cardiovascular-protective agent.

KEYWORDS: andrographolide, EA.hy926 cells, ICAM-1, NF-κB, TNF-α

INTRODUCTION

Andrographis paniculata (Burm. f) Nees (Acanthaceae), a well-known traditional medicinal plant in India, Thailand, and China, has attracted much attention recently because of its potential for clinical application. *A. paniculata* contains diterpene lactones, flavonoids, and polyphenols. Andrographolide is a major bioactive diterpene lactone in *A. paniculata*, which is concentrated in the leaves. Many studies have shown that andrographolide possesses anti-inflammatory,[1,2] antitumor,[3,4] antiviral,[5] antioxidative,[6] antihyperglycemic,[7] and hepatoprotective [8] properties. The anti-inflammatory property of andrographolide has been extensively studied both in vivo and in vitro. Andrographolide was shown to attenuate ovalbumin-induced airway inflammation in BALB/c mice through reduced expression of cytokines and chemokines.[2] In human neutrophils, andrographolide prevents reactive oxygen species (ROS) production and decreases macrophage adhesion molecule-1 (Mac-1) expression induced by *N*-formyl-methionyl-leucyl-phenylalanine (fMLP). These events lead to the inhibition of neutrophil adhesion and transmigration.[9]

Atherosclerosis is a chronic inflammatory response. A particularly important risk factor is elevated plasma low-density lipoprotein (LDL). Expression of pro-inflammatory cytokines and adhesion molecules is increased by activated endothelial cells, which are stimulated by oxidized-LDL (ox-LDL) or injury to vessel walls. Leukocyte recruitment and ox-LDL uptake stimulate the growth of plaque and further formation of fatty lesions. Reinforcement of inflammation may cause local proteolysis, plaque rupture, and thrombus formation, which lead to ischemia and infarction.[10] Cytokines and adhesion molecules both play important roles in leukocyte recruitment. During atherosclerotic progression, adhesion molecules are involved in the adhesion and transendothelial migration of leukocytes.[11] Kaufmann et al.[12] demonstrated adhesion molecule expression at atherosclerotic plaques by immunohistochemistry. Cytokines including IL-1 and TNF-α induce the expression of E-selectin, VCAM-1, and ICAM-1 through NF-κB activation in human endothelial cells.[13−15]

ICAM-1, a transmembrane glycoprotein, is regarded as an inflammatory indicator. In comparison with the other transcription factor (e.g., AP-1 and STAT) binding sites on the ICAM-1 promoter, the NF-κB binding site plays a critical role in TNF-α-induced ICAM-1 expression.[16] NF-κB is involved in the regulation of gene expression of inflammatory and immune responses. The NF-κB family comprises five members: RelA (p65), RelB, c-Rel, p50/p105 (NF-κB1), and p52/p100 (NF-κB2). NF-κB subunits are dimerized and retained in the cytoplasm with inhibitory protein, IκB. Activation of the IKK complex results in

Received: October 13, 2010
Revised: April 14, 2011
Accepted: April 14, 2011
Published: April 14, 2011

the phosphorylation of the IκB family and subsequent degradation by 26S proteasome. Free NF-κB complex then translocates to the nucleus and binds to the κB binding site of target genes.[17]

CREB binding protein (CBP)/p300 is a cofactor that recruits transcriptional machinery, such as TFIID, TFIIB, and RNA polymerase II holoenzyme.[18] Moreover, it has histone acetyltransferase activity, which changes the structure of chromatin and increases the efficiency of transactivation.[19] Competition for CBP/p300 by different transcription factors has been suggested to integrate the diverse signaling pathways.[20] In the nucleus, the transcriptional activity of NF-κB and other transcription factors such as CREB is known to be modulated by CBP/p300.[21]

It was pointed out that p65 and CREB compete for the same cofactor, CBP.[22] This raises the possibility that NF-κB-mediated gene expression is attenuated by CREB activation and that this is due to the competitive binding of CBP between CREB and p65.[23] For instance, treatment of human umbilical vascular endothelial cells (HUVECs) with forskolin reduces NF-κB-dependent gene transcription. The suppression effect of forskolin is enhanced by CREB overexpression but reversed by CBP overexpression.[23] This finding explains an increase in intracellular cAMP levels by PKA activators, including forskolin and cAMP analogues, and the reduced TNF-α production or IL-1β-induced ICAM-1 protein expression in human monocytes or primary endothelial cell cultures, respectively.[24,25]

In the present study, we investigated the effect of AP on the IKK/NF-κB signaling pathway, which mediates TNF-α-induced ICAM-1 expression in EA.hy926 cells. In addition, the role of CREB in TNF-α-induced ICAM-1 expression by andrographolide was studied. The results of this study will provide a mechanism underlying the anti-inflammatory effect of andrographolide.

MATERIALS AND METHODS

Reagents. Dulbecco's modified Eagle's medium (DMEM), RPMI-1640, RPMI-1640 (without phenol red), OPTI-MEM, 0.25% trypsin−EDTA, and penicillin/streptomycin were from GIBCO-BRL (Grand Island, NY); Hank's balanced salt solution (HBSS) and fetal bovine serum (FBS) were from HyClone (Logan, UT); andrographolide (AP) was from Calbiochem (Darmstadt, Germany); human TNF-α, sodium bicarbonate, and 3-(4,5-dimethylthiazol-2-yl)-2,5-diphenyltetrazolium bromide (MTT) were from Sigma (St. Louis, MO); Z-Leu-Leu-Leu-CHO (MG132) was from Boston Biochem (Cambridge, MA); bis-(carboxyethyl)carboxyfluorescein acetoxymethyl ester (BCECF-AM) was from Molecular Probes (Eugene, OR); anti-actin, anti-ICAM-1, anti-CREB, anti-phospho-CREB (Ser 133), anti-phospho-IκBα (Ser32/36), and anti-phospho IKKα (Ser180)/ IKKβ (Ser181) antibodies were from Cell Signaling Technology (Boston, MA); anti-IκBα and anti-IKKα/β antibodies were from Santa Cruz Biotechnology (Santa Cruz, CA); anti-p65 antibody was from BD Bioscience (San Jose, CA); fluorescein isothiocyanate-conjugated mouse anti-human ICAM-1 antibody was from Serotec Co. (Kidlington, Oxford, U.K.); and TRIzol reagent was from Invitrogen (Carlsbad, CA). The biotin-labeled double-stranded κB consensus oligonucleotide primers for electrophoretic mobility shift assay (EMSA) were synthesized by MDBio Inc. (Taipei, Taiwan). Transfection reagent Dharmafect 1, predesigned small interfering RNA (siRNA) against human CREB, and nontargeting pool were purchased from Dharmacon Research, Inc. (Lafayette, CO).

Cell Cultures. The human endothelial cell line EA.hy926 was a kind gift from Dr. T. S. Wang, Chung Shan Medical University, Taichung, Taiwan, and was cultured in DMEM supplemented with 3.7 g/L $NaHCO_3$, 10% FBS, 100 U/mL penicillin, and 100 μg/mL streptomycin at 37 °C in a 5% CO_2 humidified incubator. Human leukemia promyelocytic cells (HL-60) were purchased from Bioresources Collection and Research Center (BCRC, HsinChu, Taiwan). The HL-60 cells were cultured in T-75 tissue culture flasks in RPMI-1640 medium supplemented with 10% FBS, 100 U/mL penicillin, and 100 μg/mL streptomycin. Cells were incubated at 37 °C in a 5% CO_2 humidified incubator.

Cell Viability Assay. Cell viability was assessed by the MTT assay (see Figure S1 of the Supporting Information). The MTT assay measures the ability of viable cells to reduce a yellow 3-(4,5-dimethylthiazol-2-yl)-2,5-diphenyltetrazolium bromide to a purple formazan by mitochondrial succinate dehydrogenase. EA.hy926 cells were grown to 70−80% confluence and were then treated with different concentrations of andrographolide (0−20 μM) for 16 h followed by incubation with TNF-α (1 ng/mL) for another 6 h. Finally, the DMEM was removed, and the cells were washed with PBS. The cells were then incubated with MTT (0.5 mg/mL) in DMEM at 37 °C for an additional 3 h. The medium was removed, and isopropanol was added to dissolve the formazan. After centrifugation at 20000*g* for 5 min, the supernatant of each sample was transferred to 96-well plates, and absorbance was read at 570 nm in an ELISA reader. The absorbance in cultures treated with 0.1% DMSO was regarded as 100% cell viability.

Nuclear Extract Preparation. After each experiment, cells were washed twice with cold PBS and were then scraped from the dishes with 1000 μL of PBS. Cell homogenates were centrifuged at 2000*g* for 5 min. The supernatant was discarded, and the cell pellet was allowed to swell on ice for 15 min after the addition of 200 μL of hypotonic buffer containing 10 mM HEPES, 1 mM $MgCl_2$, 1 mM EDTA, 10 mM KCl, 0.5 mM DTT, 0.5% Nonidet P-40, 4 μg/mL leupeptin, 20 μg/mL aprotinin, and 0.2 mM PMSF. After centrifugation at 7000*g* for 15 min, pellets containing crude nuclei were resuspended in 50 μL of hypertonic buffer containing 10 mM HEPES, 400 mM KCl, 1 mM $MgCl_2$, 0.25 mM EDTA, 0.5 mM DTT, 4 μg/mL leupeptin, 20 μg/mL aprotinin, 0.2 mM PMSF, and 10% glycerol at 4 °C for 30 min. The samples were then centrifuged at 20000*g* for 15 min. The supernatant containing the nuclear proteins was collected and stored at −80 °C until the Western blotting and electrophoretic mobility shift assays.

Western Blot Analysis. After each experiment, cells were washed twice with cold PBS and were harvested in 150 μL of lysis buffer (10 mM Tris-HCl, pH 8.0, 0.1% Triton X-100, 320 mM sucrose, 5 mM EDTA, 1 mM PMSF, 1 μg/mL leupeptin, 1 μg/mL aprotinin, and 2 mM dithiothreitol). Cell homogenates were centrifuged at 14000*g* for 20 min at 4 °C. The resulting supernatant was used as a cellular protein for Western blot analysis. The preparation of nuclear extracts was described above. The total protein was analyzed by use of the Coomassie Plus protein assay reagent kit (Pierce Biotechnology Inc., Rockford, IL). Equal amounts of proteins were electrophoresed in an SDS−polyacrylamide gel, and proteins were then transferred to polyvinylidene fluoride membranes. Nonspecific binding sites on the membranes were blocked with 5% nonfat milk in 15 mM Tris/150 mM NaCl buffer (pH 7.4) at room temperature for 2 h. Membranes were probed with anti-actin, anti-ICAM-1, anti-CREB, anti-phospho-CREB (Ser 133), anti-phospho-IκBα (Ser32/36) and anti-phospho IKKα (Ser180)/IKKβ (Ser181), anti-IκBα and anti-IKKα/β, and anti-p65 antibodies. The membranes were then probed with the secondary antibody labeled with horseradish peroxidase. The bands were visualized by using an enhanced chemiluminescence kit (PerkinElmer Life Science, Boston, MA) and were scanned by a luminescent image analyzer (Fujifilm LAS-4000, Japan). The bands were quantitated with an ImageGauge (Fujifilm).

RNA Isolation and RT-PCR. Total RNA of EA.hy926 cells was extracted by using TRIzol reagent. After treatment, cells were washed twice with cold PBS and scraped with 500 μL of TRIzol reagent. Cell samples were mixed with 100 μL of chloroform and centrifuged at 11000*g* for 15 min. The supernatant was collected and mixed with 250 μL of isopropyl alcohol. After centrifugation at 12000*g* for 20 min, the

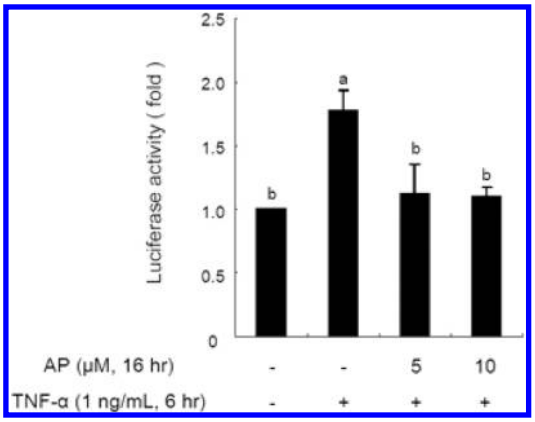

Figure 1. Andrographolide (AP) inhibits TNF-α-induced ICAM-1 promoter activity in EA.hy926 cells. Cells transfected with the pIC339 luciferase expression vector were pretreated with andrographolide for 16 h followed by incubation with TNF-α for an additional 6 h. Cells were then lysed and analyzed for luciferase activity. Luciferase activity was assayed as described under Materials and Methods. Induction is shown as an increase in the normalized luciferase activity in the treated cells relative to the control. Values are the mean ± SD of three independent experiments. Values not sharing a letter are significantly different ($p < 0.05$).

supernatant was discarded and the RNA precipitate was stored in 70% ethanol or dissolved in deionized water for quantification. We used 0.2 μg of total RNA for the synthesis of first-strand cDNA by using Moloney murine leukemia virus reverse transcriptase (Promega Co., Madison, WI) in a 20-μL final volume containing 250 ng of oligo(dT) and 40 U of RNase inhibitor. PCR was carried out in a thermocycler in a 50-μL reaction volume containing 20 μL of cDNA, BioTaq PCR buffer, 50 μM of each deoxyribonucleotide triphosphate, 1.25 mM $MgCl_2$, and 1 U of BioTaq DNA polymerase (BioLine). Oligonucleotide primers of ICAM-1 (forward, 5′-TGAAGGCCACCCCAGAGGACAAC-3′; reverse, 5′-CCCATTATGACTGCGGCTGCTGCTACC-3′) and glyceraldehyde 3-phosphate dehydrogenase (forward, 5′-CCATCACCATCTTCCAGGAG-3′; reverse, 5′-CCTGCTTCACCACCTTCTTG-3′) were designed on the basis of published sequences.[26] Amplification of ICAM-1 and GAPDH was performed by heating samples to 95 °C for 5 min and then immediately cycling 32 times through a 1-min denaturing step at 94 °C, a 1 min annealing step at 56 °C, and a 1-min elongation step at 72 °C. The glyceraldehyde 3-phosphate dehydrogenase cDNA level was used as the internal standard. PCR products were resolved in a 1% agarose gel, scanned by using a Digital Image Analyzer (Alpha Innotech), and quantitated with an ImageGauge.

ICAM-1 Expression on Cell Surfaces. The expression of ICAM-1 on plasma membranes was measured by fluorescence flow cytometry. After treatment, cells were suspended in 0.25% trypsin and centrifuged at 2000*g* for 5 min. The supernatant was discarded, and the cells were reacted with fluorescein isothiocyanate-conjugated mouse anti-human ICAM-1 antibody at 4 °C for 45 min in the dark. Cells were washed three times with cold PBS, and fluorescence was read by use of a Becton Dickinson FACSCalibur (BD Biosciences, San Jose, CA).

Monocyte Adhesion Assay. EA.hy926 cells in 12-well plates were allowed to grow to 80% confluence and were then pretreated with andrographolide for 16 h followed by incubation with 1 ng/mL TNF-α for another 6 h. Human monocytic HL-60 cells cultured in RPMI 1640 medium with 10% FBS were labeled with 1 μM BCECF-AM. At the end of andrographolide and TNF-α treatment, a total of 1×10^6 BCECF-AM-labeled HL-60 cells were added to each well, and the cells were co-incubated with EA.hy926 cells at 37 °C for 30 min. The wells were washed and filled with cell culture medium, and the plates were sealed, inverted, and centrifuged at 100*g* for 5 min to remove nonadherent HL-60 cells. Bound HL-60 cells were lysed in a 1% SDS solution, and the fluorescence intensity was determined in a fluoroscan ELISA plate reader (FLX800, Bio-Tek, Winooski, VT) with an excitation wavelength of 480 nm and an emission wavelength of 520 nm. A control study showed that fluorescence is a linear function of HL-60 cells in the range of 3000−80000 cells/well. The results are reported on the basis of the standard curve obtained.

Plasmid, Transfection, and Luciferase Assays. The ICAM-1 promoter-luciferase construct (pIC339, −339 to 0) was a gift from Dr. P. T. van der Saag (Hubrecht Laboratory, Utrecht, The Netherlands). pIC339 contains NF-κB (−187/−178), AP-1 (−284/−279), AP-2 (−48/−41), and Sp1 (−59/−53, −206/−201) binding sites.[27] EA.hy926 cells were transiently transfected with 0.1 μg of pIC339 plasmid and 0.1 μg of β-galactosidase plasmid by using 1 μL of nanofectin (PAA, Pasching, Austria) in OPTI-MEM medium for 4 h. After transfection, cells were changed to DMEM and treated with andrographolide for 16 h before being challenged with TNF-α for an additional 6 h. Cells were then washed twice with cold PBS, scraped with lysis buffer (Promega), and centrifuged at 14000*g* for 3 min. The supernatant was collected for the measurement of luciferase and β-galactosidase activities by using a Luciferase Assay Kit (Promega) according to the manufacturer's instructions. The luciferase activity of each sample was corrected on the basis of β-galactosidase activity, which was measured at 420 nm with *O*-nitrophenyl-β-D-galactopyranoside as a substrate. The value for cells treated with 0.1% DMSO (control) was set at 1.

Electrophoretic Mobility Shift Assay (EMSA). EMSA was performed according to our previous study.[28] The LightShift Chemiluminescent EMSA Kit (Pierce Chemical Co., Rockford, IL) and synthetic biotin-labeled double-stranded κB consensus oligonucleotides (forward, 5′-AGTTGAGGGGACTTTCCCAGGC-3′; reverse, 5′-GCCTGGGAAAGTCCCCTCAACT-3′) were used to measure NF-κB nuclear protein−DNA binding activity. Ten micrograms of nuclear extract, poly(dI-dC), and biotin-labeled double-stranded NF-κB oligonucleotides were mixed with the binding buffer (Chemiluminescent Nucleic Acid Detection Module, Thermo, Rockford, IL) to a final volume of 20 μL, and the mixture was incubated at 27 °C for 30 min. Unlabeled double-stranded NF-κB oligonucleotides and mutant double-stranded oligonucleotides (5′-AGTTGAGGCGACTTTCCCAGGC-3′) were used to confirm the protein-binding specificity. The nuclear protein−DNA complex was separated by electrophoresis on a 6% TBE−polyacrylamide gel and was then transferred to a Hybond-N^+ nylon membrane. The membranes were cross-linked by UV light for 10 min and were then treated with 20 μL of streptavidin−horseradish peroxidase for 20 min, and the nuclear protein−DNA bands were developed with a Chemiluminescent Substrate (Thermo). The bands were scanned by a luminescent image analyzer (Fujifilm LAS-4000).

Intracellular cAMP Measurement. After treatment, cells were washed twice with cold PBS and lysed and scraped into 200 μL of 0.1 N HCl. Cell homogenates were centrifuged at 1000*g* for 10 min. The resulting supernatant was collected for the measurement of cAMP and protein. Intracellular cAMP concentrations were measured by using the cAMP EIA kit (Cayman Chemical Co., Ann Arbor, MI). The protein content was determined by using the Coomassie Plus protein assay reagent kit. cAMP concentrations in the control are expressed as 100%, and the concentrations in the other groups were calculated in comparison with the control.

RNA Interference by Small Interfering RNA of CREB. EA.hy926 cells were cultured and allowed to grow to 80% confluence. EA.hy926 cells were transfected with CREB siRNA SMARTpool by using DharmaFECT1 transfection reagent (Thermo) according to the manufacturer's instructions. The four siRNAs against the human CREB gene are (1) GAGAGAGGUCCGUCUAAUG, (2) UAGUACAGCUGCCCAAUGG, (3) CAACUCCAAUUUACCAAAC, and (4) GCCCAGCCAUCAGUUAUUC. A nontargeting control-pool siRNA (NTC) was

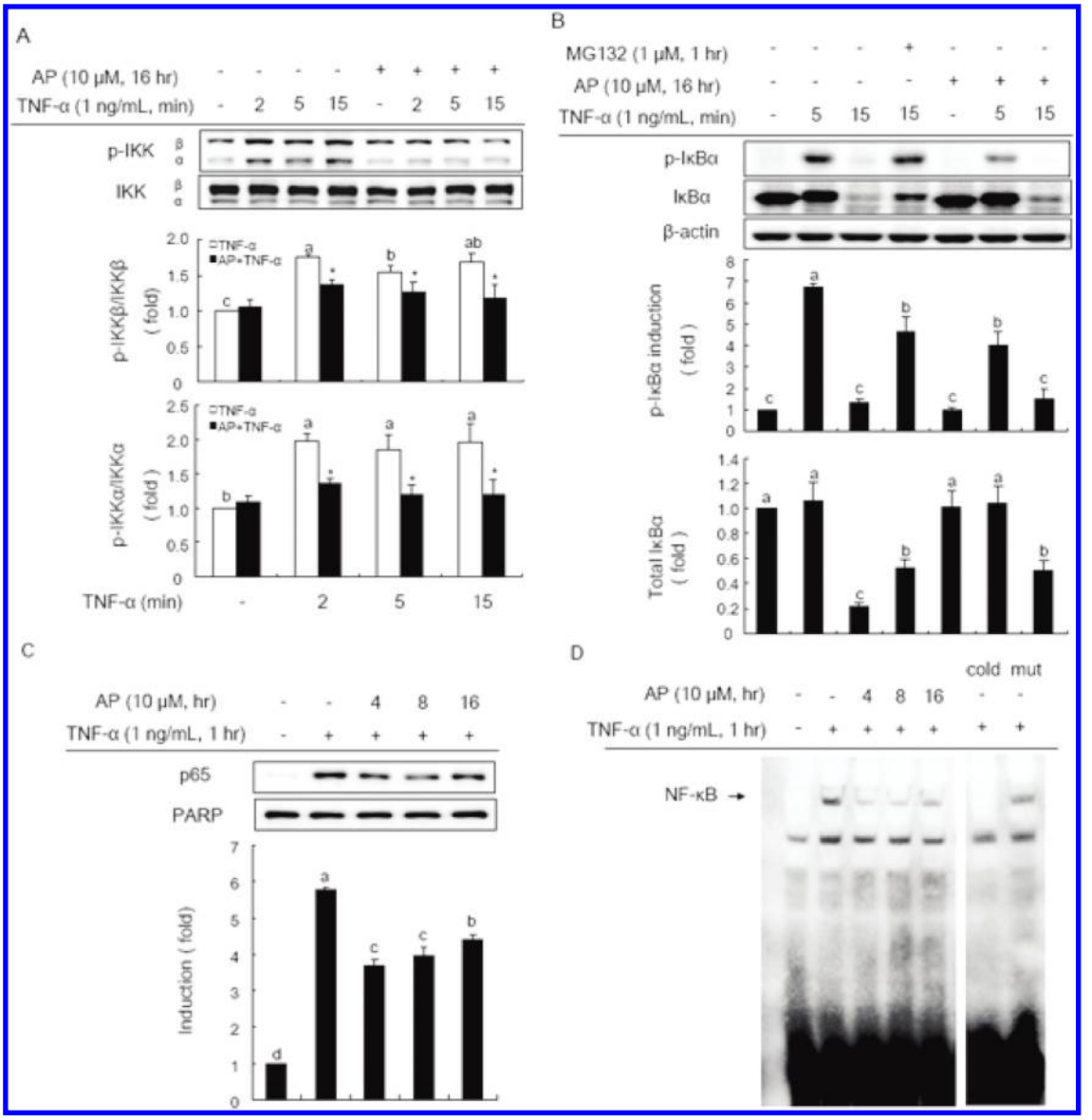

Figure 2. Andrographolide (AP) inhibits TNF-α-induced activation of NF-κB. (A) Cells were pretreated with 10 μM andrographolide for 16 h followed by incubation with 1 ng/mL TNF-α for the various time periods. Aliquots of total protein (20 μg) were used for Western blot analysis. Fold activation is shown as an increase in the normalized phosphorylation in the treated cells relative to the control. (B) Cells were pretreated with 10 μM andrographolide for 16 h or with 1 μM proteasome inhibitor, MG132, for 1 h followed by incubation with 1 ng/mL TNF-α for various time periods. Aliquots of total protein (20 μg) were used for Western blot analysis. (C) Nuclear extracts (10 μg) were used for Western blot analysis. (D) Aliquots of nuclear extracts (10 μg) were used for EMSA. One representative experiment of three independent experiments is shown. For panels A−C, the levels in control cells were set at 1. Values are the mean ± SD of three independent experiments. Values not sharing a letter are significantly different ($p < 0.05$). ∗, $p < 0.05$, indicates significant effect of andrographolide on TNF-α-induced IKKα/β phosphorylation.

also tested and was used as the negative control. After 8 h of transfection, cells were treated with andrographolide for 16 h before incubation with TNF-α for another 6 h. Cell samples were collected for Western blot analysis.

Statistical Analysis. Data were analyzed by using analysis of variance (SAS Institute, Cary, NC). The significance of the difference among mean values was determined by one-way analysis of variance followed by the Tukey's test. p values of <0.05 were taken to be statistically significant.

RESULTS

Andrographolide Inhibits TNF-α-Induced ICAM-1 Expression and HL-60 Cell Adhesion in EA.hy926 Cells. Similar to our previous study,[41] AP inhibited TNF-α-induced ICAM-1 mRNA and protein levels, its expression on the cell surface, and subsequent adhesion of HL-60 cells to EA.hy926 cells (see Figure S3 of the Supporting Information).

Andrographolide Inhibits TNF-α-Induced ICAM-1 Luciferase Reporter Activity. To investigate the role of andrographolide in TNF-α-induced ICAM-1 gene transcription, promoter activity assays were performed with a human ICAM-1 promoter-luciferase construct, pIC339 (−339 to 0). TNF-α-induced ICAM-1 promoter activation was inhibited by 5 and 10 μM andrographolide (Figure 1).

Andrographolide Inhibits TNF-α-Induced Activation of NF-κB. Several putative recognition sequences for a variety of transcriptional activators, including AP-1, retinoic acid-response

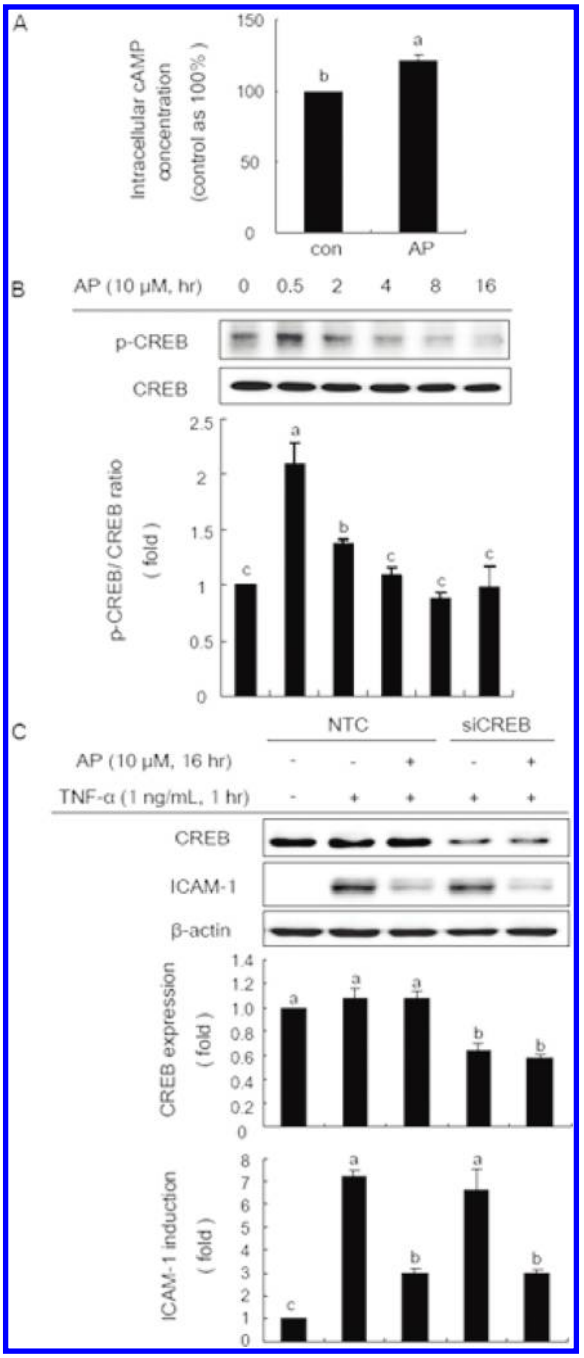

Figure 3. Andrographolide (AP) increases the intracellular cAMP concentration and induces the phosphorylation of CREB, but CREB is not involved in AP inhibition of TNF-α-induced ICAM-1 expression in EA.hy926 cells. (A) Cells were treated with 10 μM andrographolide for 30 min. (B) Cells were treated with 10 μM andrographolide for various time periods. Nuclear extracts (15 μg) were used for Western blot analysis. (C) A CREB siRNA system was used to silence CREB mRNA in cells and to create an siRNA knockdown EA.hy926 cell model. Eight hours after transfection, cells were pretreated with 10 μM andrographolide for 16 h followed by incubation with 1 ng/mL TNF-α for an additional 6 h. Aliquots of total protein (20 μg) were used for Western blot analysis. The levels in control cells were set at 1. Values are the mean ± SD of three independent experiments. Values not sharing a letter are significantly different ($p < 0.05$). One representative immunoblot from three independent experiments is shown.

element (RARE), C/EBP, NF-κB, Ets-1, interferon-stimulated response element (IRE), Sp1, and AP-2, are present in the human proximal ICAM-1 promoter-enhancer region (−346 to −24).[29] Among these, NF-κB binding to the κB binding site plays a critical role in TNF-α-induced ICAM-1 expression by activating IKKα/β. Accordingly, we next determined whether NF-κB activation was inhibited by andrographolide. As shown in Figure 2A, TNF-α induced both IKKα and IKKβ phosphorylation, and the activation of IKKα and IKKβ was significantly attenuated by andrographolide pretreatment. In addition to the activation of IKKα/β, TNF-α caused the phosphorylation and degradation of IκBα at 5 and 15 min, respectively. However, the phosphorylation induced by TNF-α was abolished by pretreatment with andrographolide, and the degradation was attenuated by pretreatment with andrographolide or MG132 (a proteasome inhibitor) (Figure 2B). To investigate the effect of andrographolide on TNF-α-induced NF-κB activation, the p65 content of the nucleus was determined by Western blotting. Nuclear translocation of p65 was induced by TNF-α, and this effect was attenuated by andrographolide pretreatment (Figure 2C). EMSA further revealed that TNF-α increased NF-κB nuclear protein−DNA complex formation and that pretreatment with andrographolide resulted in the inhibition of NF-κB nuclear protein−DNA binding activity (Figure 2D).

Andrographolide Increases the Intracellular cAMP Concentration and Induces Phosphorylation of CREB in EA.hy926 Cells. Many studies have reported that NF-κB-mediated transcription can be counteracted by activation of the cAMP/PKA/CREB signaling pathway. This effect is due to the competition for CBP between NF-κB and CREB.[23,24] Our previous study showed that andrographolide elevates intracellular cAMP and activates CREB in rat primary hepatocytes.[30] Therefore, to investigate whether cAMP and CREB were involved in the inhibition of ICAM-1 expression by andrographolide, we analyzed the intracellular cAMP concentration and CREB phosphorylation. We found that treatment with 10 μM andrographolide for 30 min resulted in a 20% increase in the intracellular cAMP concentration ($p < 0.05$) (Figure 3A) accompanied by an increase in CREB phosphorylation at 0.5 and 2 h (Figure 3B)

CREB siRNA Shows No Effect on Andrographolide Inhibition of ICAM-1 Expression in the Presence of TNF-α. To demonstrate whether competition for CBP by CREB was involved in the inhibition of andrographolide, we used CREB siRNA. Transient transfection with CREB siRNA knocked down CREB expression in EA.hy926 cells but did not affect the inhibition of ICAM-1 expression by andrographolide (Figure 3C). These results suggest that it is likely that CREB is not involved in the suppression of ICAM-1 by andrographolide.

DISCUSSION

TNF-α is a well-known pro-inflammatory cytokine that is commonly found in atherosclerotic lesions[31] and that provides cell signals that result in the activation of NF-κB. The activation of NF-κB is intimately associated with the development of inflammatory responses via up-regulation of the expression of inflammatory mediators.[32,33] Many studies have shown that the TNF-α-induced expression of pro-inflammatory cytokines (e.g., IL-6 and IL-1β)[34,35] and adhesion molecules (e.g., ICAM-1 and VCAM-1)[16,36] is dependent on NF-κB activation. The increased expression of pro-inflammatory cytokines and adhesion molecules enables T cells and endothelial cells to interact with each

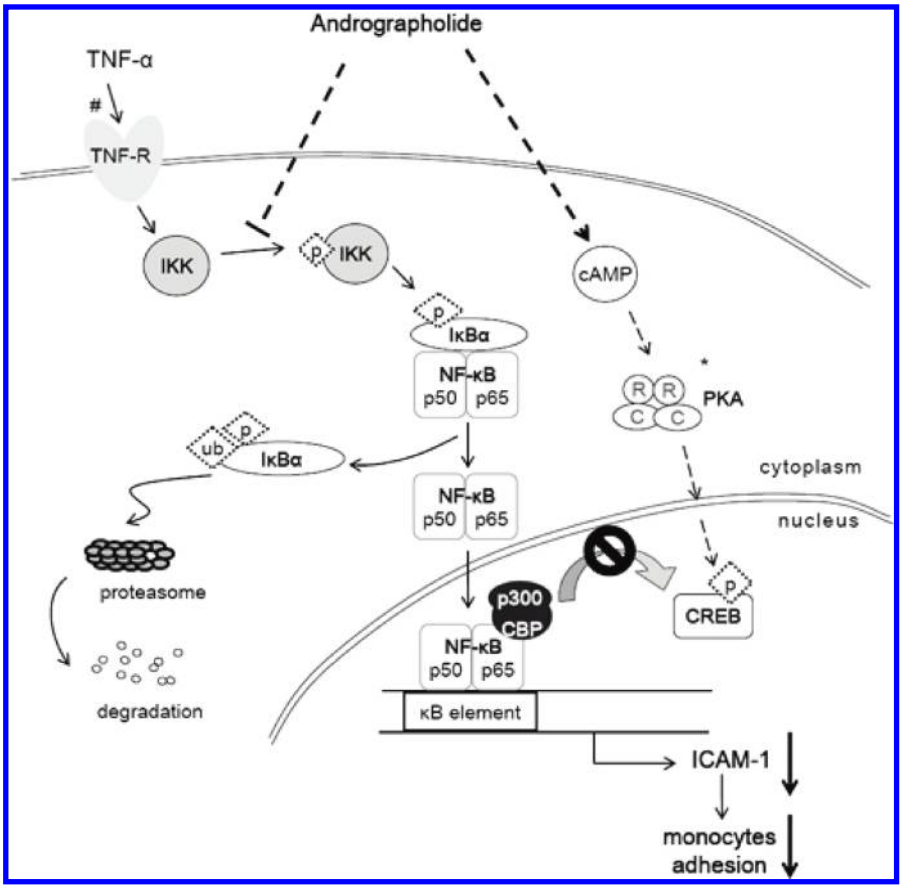

Figure 4. Model showing the pathways that mediate the inhibition of expression of ICAM-1 and adhesion of HL-60 cells to EA.hy926 cells by andrographolide under inflammatory conditions. Andrographolide inhibits TNF-α-induced IKK activation, IκBα phosphorylation and degradation, p65 nuclear translocation, and DNA binding activity of NF-κB and, eventually, suppresses ICAM-1 expression and monocyte adhesion. Activation of CREB is not involved in the inhibition of ICAM-1 expression by andrographolide, and CREB does not compete with NF-κB for CBP in the present study. #, see ref 55. ∗, see ref 56.

other. TNF-α was reported to up-regulate VCAM-1 expression via the activation of MAPK pathways in human tracheal smooth muscle cells[37] or through the PKCδ-p38 kinase-linked cascade in the lung airway epithelium.[38] TNF-α was also reported to enhance ICAM-1 expression via the activation of the phosphatidylcholine phospholipase C (PC-PLC)/diacylglycerol (DAG)/PKC pathway mediated by the TNF-α receptor p55 (TNF-R1) in well-differentiated normal human bronchial epithelial cells.[39]

Atherosclerosis is recognized to be a chronic inflammation-related disease, and the abnormal expression of adhesion molecules on vessel walls and leukocytes is involved in atherosclerotic progression.[40] The potent anti-inflammatory activity of andrographolide has been demonstrated both in vivo and in vitro.[1,2] In our previous study, we showed that andrographolide inhibits TNF-α-induced ICAM-1 expression in EA.hy926 cells and HL-60 adhesion and that these actions occur via up-regulation of heme-oxygenase (HO)-1 expression.[41] HO-1 is recognized to have both antioxidative and detoxifying properties.[42] In the present study, we examined possible mechanisms other than the induction of HO-1 expression in the inhibition of TNF-α-induced ICAM-1 expression by andrographolide. Andrographolide did not inhibit ICAM-1 expression and HL-60 adhesion to the same extent at 5 μM, and this means monocyte adhesion to endothelial cells is due to not only ICAM-1 but also any other gene expression, possibly VCAM-1. We did not use ICAM-1 siRNA to determine the role of ICAM-1 in HL-60 adhesion; however, Xie et al.[43] have demonstrated the role of ICAM-1 in monocyte adherence to basal or IL-1β-treated decidual endothelial cells by using ICAM-1 MoAb and ICAM-1 siRNA. Their results may support our data that inhibition of ICAM-1 expression partially explains the decreased HL-60 adhesion. ICAM-1 is a membrane protein, and the expression of membrane proteins is dependent on the balance between their export via the endoplasmic reticulum and Golgi apparatus to reach the plasma membrane and the membrane protein degradation.[44] It is reported that down-regulation of ICAM-1 and VCAM-1 expression in endothelial cells treated by photodynamic therapy is mediated by lysosome rather than by 26S proteosome and calpain pathways.[44] In the present study, the decreased TNF-α-induced cell surface expression of ICAM-1 by andrographolide may be the result of reduced ICAM-1 transcription and translation or enhanced cell surface ICAM-1 degradation by unidentified mechanisms (see Figure S2 of the Supporting Information).

Several signaling pathways are involved in TNF-α-mediated cellular responses. These are the IKK/NF-κB,[45] MAPK,[46] PI3K/Akt,[47] PKC,[48] and JAK/STAT[49] pathways. In addition to NF-κB, AP-1 is considered to be involved in TNF-α-induced inflammatory gene expression. TNF-α and IFN-γ treatment induces NO production and iNOS expression in C6 cells, and this action is through activation of NF-κB, AP-1, and IRF-1 transcription

factors.[50] Many phytochemicals have been shown to reduce inflammation because of their effectiveness at blocking NF-κB activation. For example, curcumin decreases the expression of ICAM-1, monocyte chemoattractant protein (MCP)-1, and IL-8 induced by TNF-α in HUVECs through the modulation of p38 and STAT-3 in addition to NF-κB and JNK.[49] Incensole acetate, an important compound in the anti-inflammatory agent *Boswellia* resin, inhibits TAK/TAB-mediated IKK activation loop phosphorylation, which results in the inhibition of cytokine and LPS-mediated NF-κB activation. Incensole acetate showed a powerful anti-inflammatory effect in a mouse inflamed paw model.[51] Lycopene, a natural carotenoid from tomato and other sources, has been shown to inhibit TNF-α-induced ICAM-1 expression in HUVECs, and this action is via attenuation of TNF-α-induced IκB phosphorylation, NF-κB expression, and NF-κB p65 translocation from the cytosol to the nucleus.[46] Carnosol, a diterpene derived from the herb rosemary, abolishes TNF-α-induced NF-κB nuclear translocation and transcriptional activity and inhibits TNF-α-induced endothelial ICAM-1 expression and monocyte adhesion.[52] In our study, we observed that TNF-α induced ICAM-1 promoter activity and that this effect was abolished by 5 and 10 μM andrographolide (Figure 1). To investigate whether the IKK/NF-κB pathway was involved in the inhibition by andrographolide, we analyzed IKKα/β phosphorylation, IκBα phosphorylation and degradation, p65 nuclear translocation, and the DNA binding activity of NF-κB. Our data clearly disclose that andrographolide inhibits TNF-α-induced IKKα/β phosphorylation (Figure 2A) and reduces the phosphorylation and degradation of IκBα (Figure 2B), p65 nuclear translocation (Figure 2C), and DNA binding activity of NF-κB (Figure 2D). Thereby, our results demonstrate that IKK is an andrographolide target in the NF-κB pathway. In a recent work, inhibition of the IKK/NF-κB signaling pathway by andrographolide was also found in human bronchial epithelial cells.[2]

Several lines of evidence suggest that the cAMP/PKA/CREB signaling pathway negatively regulates NF-κB-mediated transcription. In human airway smooth muscle cells, pretreatment with forskolin, dibutyryl cAMP, or isoproterenol inhibits TNF-α-induced ICAM-1 and VCAM-1 expression.[53] In addition, cilostazol, which increases the intracellular cAMP level, inhibits THP-1 cell adhesion to HUVECs.[54] This suppression was considered to occur because of competition between p65 and CREB for the limited amount of CBP. Parry and Mackman[23] indicated that the inhibition by forskolin was promoted by overexpression of CREB and was attenuated by overexpression of CBP in HUVECs. In our previous study, treatment with 40 μM andrographolide for 30 min dramatically elevated the intracellular cAMP concentration by 22-fold and induced phosphorylation of CREB in rat primary hepatocytes.[30] In EA.hy926 cells, we also observed the cAMP enhancing effect of andrographolide (Figure 3A), although the magnitude was not as large as that seen in rat primary hepatocytes.[30] The different results in the two cell culture systems can be attributed to the dose of andrographolide used and the different cell models examined. The increased cAMP level and CREB phosphorylation in response to andrographolide raise the possibility that the cAMP/CREB pathway may play a role in the suppression of TNF-α-induced ICAM-1 expression. Therefore, to demonstrate the role of CREB phosphorylation in ICAM-1 expression, we performed knockdown of CREB with CREB siRNA. It was interesting to note that silencing CREB expression did not change the inhibitory effect of andrographolide on TNF-α-induced ICAM-1 expression. This finding suggests that the cAMP/CREB pathway is not involved in the inhibition of TNF-α-induced NF-κB activation, and thus the expression of ICAM-1, by andrographolide.

In summary, andrographolide effectively inhibits TNF-α-induced ICAM-1 expression and monocyte adhesion in EA.hy926 cells. This inhibition is at least partially through suppression of the IKK/NF-κB signaling pathway exerted by andrographolide rather than through modulation of the cAMP/CREB pathway. Our findings are schematically presented in Figure 4.

■ ASSOCIATED CONTENT

Supporting Information. Additional figures. This material is available free of charge via the Internet at http://pubs.acs.org.

■ AUTHOR INFORMATION

Corresponding Author

*Postal address: Department of Nutrition, China Medical University, Taichung 404, Taiwan. Phone: +886 4 22053366, ext. 7520. Fax: +886 4 2206 2891. E-mail: chenhw@mail.cmu.edu.tw.

Author Contributions

‖These authors contributed equally to this work and therefore share first authorship.

Funding Sources

This work was supported by Grant CMU99-ASIA-09.

■ ABBREVIATIONS USED

AP, andrographolide; CBP, CREB binding protein; CREB, cAMP response element-binding protein; EMSA, electrophoretic mobility shift assay; HO-1, heme oxygenase 1; HUVECs, human umbilical vascular endothelial cells; ICAM-1, intercellular adhesion molecule; IκB, κB inhibitor; IKK, κB inhibitor kinase; ROS, reactive oxygen species; siRNA, small interfering RNA; TNF-α, tumor necrosis factor α.

■ REFERENCES

(1) Abu-Ghefreh, A. A.; Canatan, H.; Ezeamuzie, C. I. In vitro and in vivo anti-inflammatory effects of andrographolide. *Int. Immunopharmacol.* **2009**, *9*, 313–318.

(2) Bao, Z.; Guan, S.; Cheng, C.; Wu, S.; Wong, S. H.; Kemeny, D. M.; Leung, B. P.; Wong, W. S. A novel antiinflammatory role for andrographolide in asthma via inhibition of the nuclear factor-κB pathway. *Am. J. Respir. Crit. Care Med.* **2009**, *179*, 657–665.

(3) Jiang, C. G.; Li, J. B.; Liu, F. R.; Wu, T.; Yu, M.; Xu, H. M. Andrographolide inhibits the adhesion of gastric cancer cells to endothelial cells by blocking E-selectin expression. *Anticancer Res.* **2007**, *27*, 2439–2447.

(4) Zhao, F.; He, E. Q.; Wang, L.; Liu, K. Anti-tumor activities of andrographolide, a diterpene from *Andrographis paniculata*, by inducing apoptosis and inhibiting VEGF level. *J. Asian Nat. Prod. Res.* **2008**, *10*, 467–473.

(5) Chen, J. X.; Xue, H. J.; Ye, W. C.; Fang, B. H.; Liu, Y. H.; Yuan, S. H.; Yu, P.; Wang, Y. Q. Activity of andrographolide and its derivatives against influenza virus in vivo and in vitro. *Biol. Pharm. Bull.* **2009**, *32*, 1385–1391.

(6) Akowuah, G. A.; Zhari, I.; Mariam, A. Analysis of urinary andrographolides and antioxidant status after oral administration of *Andrographis paniculata* leaf extract in rats. *Food Chem. Toxicol.* **2008**, *46*, 3616–3620.

(7) Yu, B. C.; Hung, C. R.; Chen, W. C.; Cheng, J. T. Antihyperglycemic effect of andrographolide in streptozotocin-induced diabetic rats. *Planta Med.* **2003**, *69*, 1075–1079.

(8) Trivedi, N. P.; Rawal, U. M.; Patel, B. P. Hepatoprotective effect of andrographolide against hexachlorocyclohexane-induced oxidative injury. *Integr. Cancer Ther.* **2007**, *6*, 271–280.

(9) Shen, Y. C.; Chen, C. F.; Chiou, W. F. Andrographolide prevents oxygen radical production by human neutrophils: possible mechanism(s) involved in its anti-inflammatory effect. *Br. J. Pharmacol.* **2002**, *135*, 399–406.

(10) Hansson, G. K. Inflammation, atherosclerosis, and coronary artery disease. *N. Engl. J. Med.* **2005**, *352*, 1685–1695.

(11) Galkina, E.; Ley, K. Vascular adhesion molecules in atherosclerosis. *Arterioscler. Thromb. Vasc. Biol.* **2007**, *27*, 2292–2301.

(12) Kaufmann, B. A.; Sanders, J. M.; Davis, C.; Xie, A.; Aldred, P.; Sarembock, I. J.; Lindner, J. R. Molecular imaging of inflammation in atherosclerosis with targeted ultrasound detection of vascular cell adhesion molecule-1. *Circulation* **2007**, *116*, 276–284.

(13) Zakeri, S. M.; Meyer, H.; Meinhardt, G.; Reinisch, W.; Schrattbauer, K.; Knoefler, M.; Block, L. H. Effects of trovafloxacin on the IL-1-dependent activation of E-selectin in human endothelial cells in vitro. *Immunopharmacology* **2000**, *48*, 27–34.

(14) Lin, C. W.; Chen, L. J.; Lee, P. L.; Lee, C. I.; Lin, J. C.; Chiu, J. J. The inhibition of TNF-α-induced E-selectin expression in endothelial cells via the JNK/NF-κB pathways by highly N-acetylated chitooligosaccharides. *Biomaterials* **2007**, *28*, 1355–1366.

(15) Zhou, Z.; Connell, M. C.; MacEwan, D. J. TNFR1-induced NF-κB, but not ERK, p38MAPK or JNK activation, mediates TNF-induced ICAM-1 and VCAM-1 expression on endothelial cells. *Cell Signal.* **2007**, *19*, 1238–1248.

(16) Oh, J. H.; Park, E. J.; Park, J. W.; Lee, J.; Lee, S. H.; Kwon, T. K. A novel cyclin-dependent kinase inhibitor down-regulates tumor necrosis factor-α (TNF-α)-induced expression of cell adhesion molecules by inhibition of NF-κB activation in human pulmonary epithelial cells. *Int. Immunopharmacol.* **2010**, *10*, 572–579.

(17) Hayden, M. S.; Ghosh, S. Signaling to NF-κB. *Genes Dev.* **2004**, *18*, 2195–2224.

(18) Kim, T. K.; Kim, T. H.; Maniatis, T. Efficient recruitment of TFIIB and CBP-RNA polymerase II holoenzyme by an interferon-β enhanceosome in vitro. *Proc. Natl. Acad. Sci. U.S.A.* **1998**, *95*, 12191–12196.

(19) Vo, N.; Goodman, R. H. CREB-binding protein and p300 in transcriptional regulation. *J. Biol. Chem.* **2001**, *276*, 13505–13508.

(20) Gerritsen, M. E.; Williams, A. J.; Neish, A. S.; Moore, S.; Shi, Y.; Collins, T. CREB binding protein/p300 are transcriptional coactivators of p65. *Proc. Natl. Acad. Sci. U.S.A.* **1997**, *94*, 2927–2932.

(21) Chen, L. F.; Greene, W. C. Shaping the nuclear action of NF-κB. *Nat. Rev. Mol. Cell Biol.* **2004**, *5*, 392–401.

(22) Sheppard, K. A.; Rose, D. W.; Haque, Z. K.; Kurokawa, R.; McInerney, E.; Westin, S.; Thanos, D.; Rosenfeld, M. G.; Glass, C. K.; Collins, T. Transcriptional activation by NF-κB requires multiple coactivators. *Mol. Cell. Biol.* **1999**, *19*, 6367–6378.

(23) Parry, G. C.; Mackman, N. Role of cyclic AMP response element-binding protein in cyclic AMP inhibition of NF-κB-mediated transcription. *J. Immunol.* **1997**, *159*, 5450–5456.

(24) Shames, B. D.; McIntyre, R. C., Jr.; Bensard, D. D.; Pulido, E. J.; Selzman, C. H.; Reznikov, L. L.; Harken, A. H.; Meng, X. Suppression of tumor necrosis factor α production by cAMP in human monocytes: dissociation with mRNA level and independent of interleukin-10. *J. Surg. Res.* **2001**, *99*, 187–193.

(25) Balyasnikova, I. V.; Pelligrino, D. A.; Greenwood, J.; Adamson, P.; Dragon, S.; Raza, H.; Galea, E. Cyclic adenosine monophosphate regulates the expression of the intercellular adhesion molecule and the inducible nitric oxide synthase in brain endothelial cells. *J. Cereb. Blood Flow Metab.* **2000**, *20*, 688–699.

(26) Meagher, L.; Mahiouz, D.; Sugars, K.; Burrows, N.; Norris, P.; Yarwood, H.; Becker-Andre, M.; Haskard, D. O. Measurement of mRNA for E-selectin, VCAM-1 and ICAM-1 by reverse transcription and the polymerase chain reaction. *J. Immunol. Methods* **1994**, *175*, 237–246.

(27) van de Stolpe, A.; Caldenhoven, E.; Stade, B. G.; Koenderman, L.; Raaijmakers, J. A.; Johnson, J. P.; van der Saag, P. T. 12-*O*-tetradecanoylphorbol-13-acetate- and tumor necrosis factor α-mediated induction of intercellular adhesion molecule-1 is inhibited by dexamethasone. Functional analysis of the human intercellular adhesion molecular-1 promoter. *J. Biol. Chem.* **1994**, *269*, 6185–6192.

(28) Cheng, W. L.; Lii, C. K.; Chen, H. W.; Lin, T. H.; Liu, K. L. Contribution of conjugated linoleic acid to the suppression of inflammatory responses through the regulation of the NF-κB pathway. *J. Agric. Food Chem.* **2004**, *52*, 71–78.

(29) Huang, W. C.; Chen, C. C. Akt phosphorylation of p300 at Ser-1834 is essential for its histone acetyltransferase and transcriptional activity. *Mol. Cell. Biol.* **2005**, *25*, 6592–6602.

(30) Yang, A. J.; Li, C. C.; Lu, C. Y.; Liu, K. L.; Tsai, C. W.; Lii, C. K.; Chen, H. W. Activation of the cAMP/CREB/inducible cAMP early repressor pathway suppresses andrographolide-induced gene expression of the π class of glutathione S-transferase in rat primary hepatocytes. *J. Agric. Food Chem.* **2010**, *58*, 1993–2000.

(31) Sana, T. R.; Janatpour, M. J.; Sathe, M.; McEvoy, L. M.; McClanahan, T. K. Microarray analysis of primary endothelial cells challenged with different inflammatory and immune cytokines. *Cytokine* **2005**, *29*, 256–269.

(32) Ghosh, S.; May, M. J.; Kopp, E. B. NF-κ B and Rel proteins: evolutionarily conserved mediators of immune responses. *Annu. Rev. Immunol.* **1998**, *16*, 225–260.

(33) Rahman, I.; MacNee, W. Role of transcription factors in inflammatory lung diseases. *Thorax* **1998**, *53*, 601–612.

(34) Ammit, A. J.; Lazaar, A. L.; Irani, C.; O'Neill, G. M.; Gordon, N. D.; Amrani, Y.; Penn, R. B.; Panettieri, R. A., Jr. Tumor necrosis factor-α-induced secretion of RANTES and interleukin-6 from human airway smooth muscle cells: modulation by glucocorticoids and β-agonists. *Am. J. Respir. Cell Mol. Biol.* **2002**, *26*, 465–474.

(35) Turner, N. A.; Mughal, R. S.; Warburton, P.; O'Regan, D. J.; Ball, S. G.; Porter, K. E. Mechanism of TNFα-induced IL-1α, IL-1β and IL-6 expression in human cardiac fibroblasts: effects of statins and thiazolidinediones. *Cardiovasc. Res.* **2007**, *76*, 81–90.

(36) Chen, C. C.; Rosenbloom, C. L.; Anderson, D. C.; Manning, A. M. Selective inhibition of Eselectin, vascular cell adhesion molecule-1, and intercellular adhesion molecule-1 expression by inhibitors of I κ B-α phosphorylation. *J. Immunol.* **1995**, *155*, 3538–3545.

(37) Lee, C. W.; Lin, W. N.; Lin, C. C.; Luo, S. F.; Wang, J. S.; Pouyssegur, J.; Yang, C. M. Transcriptional regulation of VCAM-1 expression by tumor necrosis factor-α in human tracheal smooth muscle cells: involvement of MAPKs, NF-κB, p300, and histone acetylation. *J. Cell. Physiol.* **2006**, *207*, 174–186.

(38) Woo, C. H.; Lim, J. H.; Kim, J. H. VCAM-1 upregulation via PKCδ-p38 kinase-linked cascade mediates the TNF-α-induced leukocyte adhesion and emigration in the lung airway epithelium. *Am. J. Physiol. Lung Cell. Mol. Physiol.* **2005**, *288*, L307–L316.

(39) Krunkosky, T. M.; Fischer, B. M.; Martin, L. D.; Jones, N.; Akley, N. J.; Adler, K. B. Effects of TNF-α on expression of ICAM-1 in human airway epithelial cells in vitro. Signaling pathways controlling surface and gene expression. *Am. J. Respir. Cell Mol. Biol.* **2000**, *22*, 685–692.

(40) Reiss, Y.; Engelhardt, B. T cell interaction with ICAM-1-deficient endothelium in vitro: transendothelial migration of different T cell populations is mediated by endothelial ICAM-1 and ICAM-2. *Int. Immunol.* **1999**, *11*, 1527–1539.

(41) Yu, A. L.; Lu, C. Y.; Wang, T. S.; Tsai, C. W.; Liu, K. L.; Cheng, Y. P.; Chang, H. C.; Lii, C. K.; Chen, H. W. Induction of heme oxygenase 1 and inhibition of tumor necrosis factor α-induced intercellular adhesion molecule expression by andrographolide in EA.hy926 cells. *J. Agric. Food Chem.* **2010**, *58*, 7641–7648.

(42) Kim, K. M.; Jung, D. H.; Jang, D. S.; Kim, Y. S.; Kim, J. M.; Kim, H. N.; Surh, Y. J.; Kim, J. S. Puerarin suppresses AGEs-induced inflammation in mouse mesangial cells: a possible pathway through

the induction of heme oxygenase-1 expression. *Toxicol. Appl. Pharmacol.* **2010**, *244*, 106–113.

(43) Xie, L.; Galettis, A.; Morris, J.; Jackson, C.; Twigg, S. M.; Gallery, E. D. Intercellular adhesion molecule-1 (ICAM-1) expression is necessary for monocyte adhesion to the placental bed endothelium and is increased in type 1 diabetic human pregnancy. *Diabetes Metab. Res. Rev.* **2008**, *24*, 294–300.

(44) Volanti, C.; Gloire, G.; Vanderplasschen, A.; Jacobs, N.; Habraken, Y.; Piette, J. Downregulation of ICAM-1 and VCAM-1 expression in endothelial cells treated by photodynamic therapy. *Oncogene* **2004**, *23*, 8649–8658.

(45) Spiecker, M.; Lorenz, I.; Marx, N.; Darius, H. Tranilast inhibits cytokine-induced nuclear factor κB activation in vascular endothelial cells. *Mol. Pharmacol.* **2002**, *62*, 856–863.

(46) Hung, C. F.; Huang, T. F.; Chen, B. H.; Shieh, J. M.; Wu, P. H.; Wu, W. B. Lycopene inhibits TNF-α-induced endothelial ICAM-1 expression and monocyte-endothelial adhesion. *Eur. J. Pharmacol.* **2008**, *586*, 275–282.

(47) Oh, J. H.; Kwon, T. K. Withaferin A inhibits tumor necrosis factor-α-induced expression of cell adhesion molecules by inactivation of Akt and NF-κB in human pulmonary epithelial cells. *Int. Immunopharmacol.* **2009**, *9*, 614–619.

(48) Min, J. K.; Kim, Y. M.; Kim, S. W.; Kwon, M. C.; Kong, Y. Y.; Hwang, I. K.; Won, M. H.; Rho, J.; Kwon, Y. G. TNF-related activation-induced cytokine enhances leukocyte adhesiveness: induction of ICAM-1 and VCAM-1 via TNF receptor-associated factor and protein kinase C-dependent NF-κB activation in endothelial cells. *J. Immunol.* **2005**, *175*, 531–540.

(49) Kim, Y. S.; Ahn, Y.; Hong, M. H.; Joo, S. Y.; Kim, K. H.; Sohn, I. S.; Park, H. W.; Hong, Y. J.; Kim, J. H.; Kim, W.; Jeong, M. H.; Cho, J. G.; Park, J. C.; Kang, J. C. Curcumin attenuates inflammatory responses of TNF-α-stimulated human endothelial cells. *J. Cardiovasc. Pharmacol.* **2007**, *50*, 41–49.

(50) Do, H.; Pyo, S.; Sohn, E. H. Suppression of iNOS expression by fucoidan is mediated by regulation of p38 MAPK, JAK/STAT, AP-1 and IRF-1, and depends on up-regulation of scavenger receptor B1 expression in TNF-α- and IFN-γ-stimulated C6 glioma cells. *J. Nutr. Biochem.* **2009**, *21*, 671–679.

(51) Moussaieff, A.; Shohami, E.; Kashman, Y.; Fride, E.; Schmitz, M. L.; Renner, F.; Fiebich, B. L.; Munoz, E.; Ben-Neriah, Y.; Mechoulam, R. Incensole acetate, a novel anti-inflammatory compound isolated from *Boswellia* resin, inhibits nuclear factor-κ B activation. *Mol. Pharmacol.* **2007**, *72*, 1657–1664.

(52) Lian, K. C.; Chuang, J. J.; Hsieh, C. W.; Wung, B. S.; Huang, G. D.; Jian, T. Y.; Sun, Y. W. Dual mechanisms of NF-κB inhibition in carnosol-treated endothelial cells. *Toxicol. Appl. Pharmacol.* **2010**, *245*, 21–35.

(53) Panettieri, R. A., Jr.; Lazaar, A. L.; Pure, E.; Albelda, S. M. Activation of cAMP-dependent pathways in human airway smooth muscle cells inhibits TNF-α-induced ICAM-1 and VCAM-1 expression and T lymphocyte adhesion. *J. Immunol.* **1995**, *154*, 2358–2365.

(54) Mori, D.; Ishii, H.; Kojima, C.; Nitta, N.; Nakajima, K.; Yoshida, M. Cilostazol inhibits monocytic cell adhesion to vascular endothelium via upregulation of cAMP. *J. Atheroscler. Thromb.* **2007**, *14*, 213–218.

(55) Ea, C. K.; Deng, L.; Xia, Z. P.; Pineda, G.; Chen, Z. J. Activation of IKK by TNFα requires site-specific ubiquitination of RIP1 and polyubiquitin binding by NEMO. *Mol. Cell* **2006**, *22*, 245–257.

(56) Gonzalez, G. A.; Montminy, M. R. Cyclic AMP stimulates somatostatin gene transcription by phosphorylation of CREB at serine 133. *Cell* **1989**, *59*, 675–680.